ANNUAL REVIEWS

Annual Review of Nuclear and Particle Science

Future Circular Colliders

M. Benedikt,[1] A. Blondel,[1] P. Janot,[1] M. Klein,[2] M. Mangano,[1] M. McCullough,[1] V. Mertens,[1] K. Oide,[1] W. Riegler,[1] D. Schulte,[1] and F. Zimmermann[1]

[1]CERN, 1211 Geneva 23, Switzerland; email: michael.benedikt@cern.ch

[2]Department of Physics, University of Liverpool, Liverpool L69 3BX, United Kingdom

Annu. Rev. Nucl. Part. Sci. 2019. 69:389–415

First published as a Review in Advance on August 6, 2019

The *Annual Review of Nuclear and Particle Science* is online at nucl.annualreviews.org

https://doi.org/10.1146/annurev-nucl-101918-023748

Copyright © 2019 by Annual Reviews. All rights reserved

ANNUAL REVIEWS CONNECT

www.annualreviews.org

- Download figures
- Navigate cited references
- Keyword search
- Explore related articles
- Share via email or social media

Keywords

high-energy physics, energy frontier, luminosity frontier, lepton collider, hadron collider, Higgs physics, electroweak phase transition, dark matter

Abstract

After 10 years of physics at the Large Hadron Collider (LHC), the particle physics landscape has greatly evolved. Today, a staged Future Circular Collider (FCC), consisting of a luminosity-frontier highest-energy electron–positron collider (FCC-ee) followed by an energy-frontier hadron collider (FCC-hh), promises the most far-reaching physics program for the post-LHC era. FCC-ee will be a precision instrument used to study the *Z*, *W*, Higgs, and top particles, and will offer unprecedented sensitivity to signs of new physics. Most of the FCC-ee infrastructure could be reused for FCC-hh, which will provide proton–proton collisions at a center-of-mass energy of 100 TeV and could directly produce new particles with masses of up to several tens of TeV. This collider will also measure the Higgs self-coupling and explore the dynamics of electroweak symmetry breaking. Thermal dark matter candidates will be either discovered or conclusively ruled out by FCC-hh. Heavy-ion and electron–proton collisions (FCC-eh) will further contribute to the breadth of the overall FCC program. The integrated FCC infrastructure will serve the particle physics community through the end of the twenty-first century. This review combines key contents from the first three volumes of the FCC *Conceptual Design Report*.

Contents

1. INTRODUCTION

The particle physics landscape has evolved significantly during 10 years of physics at the Large Hadron Collider (LHC). Today, an integrated Future Circular Collider (FCC) program, consisting of a luminosity-frontier highest-energy lepton collider followed by an energy-frontier hadron collider, promises the most far-reaching particle physics program that foreseeable technology can deliver. This review summarizes the eight key components of the FCC physics program, the machine designs of the lepton and hadron colliders, the civil engineering, and the implementation timeline.

2. PHYSICS OPPORTUNITIES

The legacy of the first phase of the LHC physics program includes (*a*) the discovery of the Higgs boson and the start of a new phase of detailed studies of its properties, aimed at revealing the deep origin of electroweak (EW) symmetry breaking (EWSB); (*b*) the indication that signals of new physics around the TeV scale are, at best, elusive; and (*c*) the rapid advance of theoretical calculations, whose constant progress and reliability inspire confidence in the key role of ever-improving precision measurements spanning from the Higgs to the flavor sectors. Last but not least, the success of the LHC has been made possible by the extraordinary achievements of the accelerator and of the detectors, whose performance is exceeding all expectations. Housed in

a 100-km-long tunnel, the FCC will build on this legacy and on the experience of previous or present circular colliders (LEP, HERA, the Tevatron, and the *B* factories).

The e^+e^- collider (FCC-ee) will operate at multiple center-of-mass energies $\sqrt{s}$ between 90 and 365 GeV, producing 5×10^{12} Z^0 bosons, 10^8 WW pairs, more than 10^6 Higgs bosons, and more than 10^6 $t\bar{t}$ pairs. The 100 TeV proton–proton collider (FCC-hh) is designed to collect a total luminosity of 20 ab^{-1}, corresponding to the production of, for instance, more than 10^{10} Higgs bosons. FCC-hh could also be operated with heavy ions (e.g., Pb+Pb at $\sqrt{s_{NN}} = 39$ TeV). The FCC-eh, with 50 TeV proton beams colliding with 60 GeV electrons from an energy-recovery linac, is an option that could generate ~2 ab^{-1} of 3.5 TeV electron–proton collisions.

The integrated FCC program has set highly ambitious performance goals for its accelerators and experiments. For example, it will:

1. uniquely map the properties of the Higgs and EW gauge bosons, pinning down their interactions with an accuracy that is order(s) of magnitude better than today, and acquiring sensitivity to, for instance, the processes that, during the time span from 10^{-12} and 10^{-10} s after the Big Bang, led to the creation of today's Higgs vacuum field;
2. improve by close to an order of magnitude the discovery reach for new particles at the highest masses and by several orders of magnitude the sensitivity to rare or elusive phenomena at the EW scale and below, such as those related to the generation of neutrino masses. In particular, the search for dark matter (DM) at FCC could reveal, or conclusively exclude, DM candidates belonging to large classes of models, such as thermal weakly interacting massive particles (WIMPs); and
3. probe energy scales beyond the direct kinematic reach via an extensive campaign of precision measurements sensitive to tiny deviations from Standard Model (SM) behavior. The precision will benefit from the unique center-of-mass energy calibration of FCC-ee, from event statistics (for each collider, typically several orders of magnitude larger than anything attainable before the FCC), improved theoretical calculations, synergies within the program [e.g., precise α_s and parton distribution functions (PDFs) provided to FCC-hh by FCC-ee and FCC-eh, respectively], and suitable detector performance.

A complete overview of the FCC physics potential is available elsewhere (1–3). The remainder of this section highlights some of the most significant findings that, in addition to setting targets for the FCC achievements, have driven the choice of the collider parameters (energy, luminosity) and their operation plans, and contributed to the definition of the detectors. The following subsections discuss the FCC physics potential. Selected physics highlights are compiled in the sidebar titled FCC Physics, and accelerator highlights in the sidebar titled FCC Accelerators.

Dark matter (DM): approximately 85% of the matter in the Universe has not yet been discovered; this amount of DM is required to explain the stability of many of the observed galaxies as well as numerous astronomical measurements, including gravitational lensing effects and observations of the cosmic microwave background

FCC PHYSICS

Thanks to its internal synergies and complementarity, the integrated FCC program appears to be the most powerful future facility for a thorough examination of the Higgs boson and of EWSB. The FCC should conclusively probe new states required by a strong first-order EW phase transition. The FCC will also cover the full mass range for the discovery, or definite exclusion, of thermal WIMP DM candidates. In addition, the FCC will have a broad, and in most cases unique, reach for less-than-weakly-coupled particles. The FCC-ee lepton collider operation in the Z boson resonance is particularly fertile for such discoveries. Collisions of heavy ions at the energies and luminosities of the FCC-hh hadron collider will open new avenues in the study of the collective properties of quarks and gluons. The FCC-eh lepton–hadron collider would resolve the parton structure of the proton in an unprecedented range of x and Q^2 to high accuracy, providing a per mille accurate measurement of the strong coupling constant.

FCC ACCELERATORS

The FCC-ee accelerators will produce Z, W, and Higgs bosons and top quarks at outstanding rates. The superconducting radio-frequency system of the FCC-ee is optimized for each operating point, guaranteeing peak performance throughout and permitting staged construction. The FCC-hh accelerator is designed to provide proton–proton collisions with a center-of-mass energy of 100 TeV and an integrated luminosity of ~20 ab^{-1} in each of the two main experiments over 25 years of operation. The overall project duration for implementation and operation of the integrated FCC is approximately 7 decades.

2.1. Higgs Studies

High-Luminosity LHC (HL-LHC): the approved luminosity upgrade of the LHC, designed to deliver a total of 3 ab^{-1} by the late 2030s

The achievements and prospects of the LHC Higgs program herald a new era in which the Higgs boson is moving from being the object of a search to becoming an exploration tool. The FCC is positioning itself as the most powerful heir to the future LHC Higgs legacy. On one hand, it will extend the range of measurable Higgs boson properties (e.g., its elusive $H \to gg, c\bar{c}$ decays, its total width, and its self-coupling), allowing more incisive and model-independent determinations of its couplings. On the other hand, the combination of superior precision and energy reach provides a framework in which indirect and direct probes of new physics complement one another and cooperate to characterize the nature of possible discoveries.

The FCC-ee will measure Higgs production inclusively, from its presence as a recoil to the Z boson in 10^6 $e^+e^- \to ZH$ events. This will allow the absolute measurement of the Higgs coupling to the Z boson, which is the starting point for model-independent determination of its total width, and thus of its other couplings through branching-ratio measurements. FCC-ee will measure the leading Higgs couplings to SM particles (denoted g_{HXX} for particle X) with subpercent precision. **Table 1** presents the precisions. To obtain the fit to the High-Luminosity LHC (HL-LHC)

Table 1 Precisions determined in the κ framework on the Higgs boson couplings and total decay width, as expected from the FCC-ee data, and compared with those from the HL-LHC (1, 4)[a]

Collider	HL-LHC	FCC-ee			FCC-eh
Luminosity (ab^{-1})	3	5 at 240 GeV	+1.5 at 365 GeV	+HL-LHC	2
Years	25	3	+4	NA	20
$\delta\Gamma_H/\Gamma_H$ (%)	SM	2.7	1.3	1.1	SM
$\delta g_{HZZ}/g_{HZZ}$ (%)	1.5	0.2	0.17	0.16	0.43
$\delta g_{HWW}/g_{HWW}$ (%)	1.7	1.3	0.43	0.40	0.26
$\delta g_{Hbb}/g_{Hbb}$ (%)	3.7	1.3	0.61	0.56	0.74
$\delta g_{Hcc}/g_{Hcc}$ (%)	SM	1.7	1.21	1.18	1.35
$\delta g_{Hgg}/g_{Hgg}$ (%)	2.5	1.6	1.01	0.90	1.17
$\delta g_{H\tau\tau}/g_{H\tau\tau}$ (%)	1.9	1.4	0.74	0.67	1.10
$\delta g_{H\mu\mu}/g_{H\mu\mu}$ (%)	4.3	10.1	9.0	3.8	NA
$\delta g_{H\gamma\gamma}/g_{H\gamma\gamma}$ (%)	1.8	4.8	3.9	1.3	2.3
$\delta g_{Htt}/g_{Htt}$ (%)	3.4	None	None	3.1	1.7
BR_{EXO} (%)	SM	<1.2	<1.0	<1.0	NA

[a]All numbers indicate 68% CL sensitivities, except for the last line, which gives the 95% CL sensitivity on the exotic branching fraction, accounting for final states that cannot be tagged as SM decays. The fits to the HL-LHC or FCC-eh projected errors alone require model assumptions to be made: Here, the total width is set to its SM value, thereby reducing the errors in comparison to the model-independent fit using FCC-ee.
Abbreviations: FCC, Future Circular Collider; FCC-ee, FCC electron–positron collider; FCC-eh, FCC electron–proton collider; HL-LHC, High-Luminosity Large Hadron Collider; NA, not applicable; SM, Standard Model.

Table 2 Target precision at FCC-hh for the parameters relative to the measurement of various Higgs decays, of ratios thereof, and of the Higgs self-coupling (1)[a]

Observable	Parameter	Precision (stat.)	Precision (stat.+syst.+lumi.)
$\mu = \sigma(H) \times B(H \to \gamma\gamma)$	$\delta\mu/\mu$	0.10%	1.45%
$\mu = \sigma(H) \times B(H \to \mu\mu)$	$\delta\mu/\mu$	0.28%	1.22%
$\mu = \sigma(H) \times B(H \to \mu\mu\mu\mu)$	$\delta\mu/\mu$	0.18%	1.85%
$\mu = \sigma(H) \times B(H \to \gamma\mu\mu)$	$\delta\mu/\mu$	0.55%	1.61%
$\mu = \sigma(HH) \times B(H \to \gamma\gamma)B(H \to b\bar{b})$	$\delta\lambda/\lambda$	5.00%	7.00%
$R = B(H \to \mu\mu)/B(H \to \mu\mu\mu\mu)$	$\delta R/R$	0.33%	1.30%
$R = B(H \to \gamma\gamma)/B(H \to ee\mu\mu)$	$\delta R/R$	0.17%	0.80%
$R = B(H \to \gamma\gamma)/B(H \to \mu\mu)$	$\delta R/R$	0.29%	1.38%
$R = B(H \to \mu\mu\gamma)/B(H \to \mu\mu)$	$\delta R/R$	0.58%	1.82%
$R = \sigma(t\bar{t}H) \times B(H \to b\bar{b})/\sigma(t\bar{t}Z) \times B(Z \to b\bar{b})$	$\delta R/R$	1.05%	1.90%
$B(H \to$ invisible$)$	B at 95% CL	1×10^{-4}	2.5×10^{-4}

[a]Note that Lagrangian couplings have a precision that is typically half of what is shown here, since all rates and branching ratios depend quadratically on the couplings.
Abbreviation: FCC-hh, Future Circular Collider hadron collider.

projections alone (first column of **Table 1**) requires assumptions: Here, the branching ratios into $c\bar{c}$ and into exotic particles (and those not indicated in the table) are set to their SM values. The FCC-ee accuracies are subdivided into three categories. The first subcolumn gives the results of the fit expected with 5 ab^{-1} at 240 GeV, the second subcolumn includes the additional 1.5 ab^{-1} at $\sqrt{s} = 365$ GeV, and the last subcolumn shows the result of the combined fit with the HL-LHC. Similar to the HL-LHC, the fit to the FCC-eh projections alone requires an assumption: In this case, the total width is set to its SM value, but in practice it will be taken to be the value measured by the FCC-ee.

The FCC-ee will also provide a first step toward the measurement of the Higgs self-coupling to 32%. Because FCC-ee will remove the model dependence, a fully complementary program will be possible at FCC-hh and FCC-eh to complete the picture of Higgs boson properties. This program will include the percent-level measurement of rare Higgs decays such as $H \to \gamma\gamma, \mu\mu, Z\gamma$; the detection of invisible decays ($H \to \nu\nu\nu\nu$); the measurement of the g_{Htt} coupling with percent-level precision; and the measurement of the Higgs self-coupling to 5–7% (as shown for FCC-hh in **Table 2**).

The Higgs couplings to all gauge bosons and to the charged fermions of the second and third generations, except the s quark, will be known with a precision ranging from a few per mille to ~1%. In addition, the prospect of measuring, or at least strongly constraining, the couplings to the three lightest quarks and to the electron by a special FCC-ee run at $\sqrt{s} = m_H$ is being evaluated. The synergies among all components of the FCC Higgs program are underscored by a global fit of Higgs parameters (**Figure 1**), which is discussed in fuller detail in Reference 1. Finally, the tagged $H \to gg$ channel at FCC-ee will offer an unprecedented sample of pure high-energy gluons.

2.2. Electroweak Precision Measurements

As proven by the discoveries that led to the consolidation of the SM, EW precision observables (EWPOs) can play a key role in establishing the existence of new physics and guiding its theoretical interpretation. We anticipate that this will continue to be the case long after the HL-LHC, and

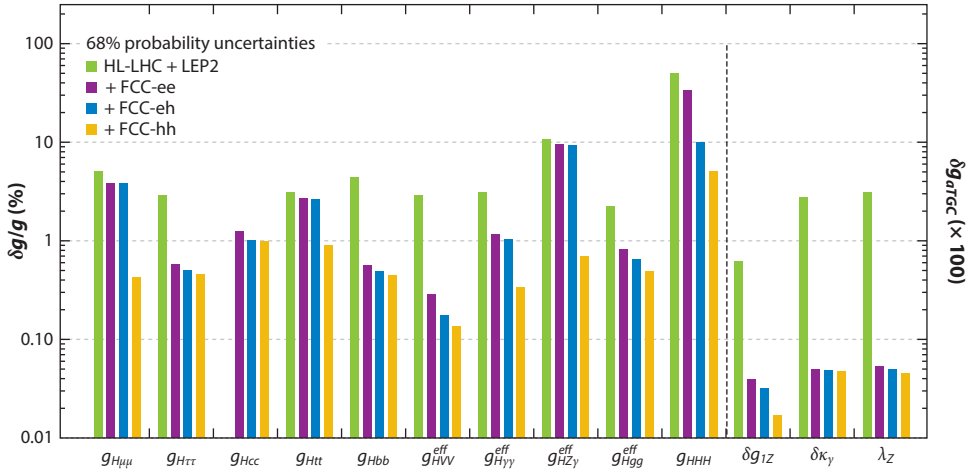

Figure 1

1σ precision reach at the FCC on the effective single-Higgs couplings, Higgs self-coupling, and anomalous triple-gauge couplings in the effective field theory framework. Absolute precision in the electroweak measurements is assumed. The different bars illustrate the improvements that would be possible by combining each FCC stage with the previous knowledge at that time (1) (precisions at each FCC stage considered individually, shown in **Tables 1** and **2** in the κ framework, are quite different). Abbreviations: FCC, Future Circular Collider; FCC-ee, FCC electron–positron collider; FCC-eh, FCC electron–proton collider; FCC-hh, FCC hadron collider; HL-LHC, High-Luminosity Large Hadron Collider; LEP2, Large Electron–Positron Collider.

we expect the FCC to lead progress in precision measurements, as improved precision equates to discovery potential.

The broad set of EWPOs accessible to FCC-ee, thanks to immense statistics at the various beam energies and to the exquisite center-of-mass energy calibration, will give it access to various possible sources and manifestations of new physics. Direct effects could occur because of the existence of a new interaction such as a Z' or W' boson, which could mix or interfere with known ones. New weakly coupled particles can affect the W, Z, or photon propagators via loops, producing flavor-independent corrections to the relation between the Z mass and the W mass or the relation between the Z mass and the effective weak mixing angle, or the loop corrections can occur as vertex corrections, leading to flavor-dependent effects (as is the case in the SM for, e.g., the $Z \to b\bar{b}$ couplings). The measurements above the $t\bar{t}$ production threshold, directly involving the top quark, as well as precision measurements of production and decays of $10^{11}\,\tau$ particles and 2×10^{12} b quarks, will further enrich this program. **Table 3** summarizes the target precision for EWPOs at FCC-ee.

The FCC-hh will achieve indirect sensitivity to new physics by exploiting its high energy, benefiting from the ability to achieve unprecedented precision in proton–proton collisions, as proven by the LHC. EW observables, such as high-mass lepton or gauge boson pairs, have a reach in the multi-TeV mass range (**Figure 2**). Their measurement could expose deviations that, despite the lower precision of FCC-hh with regard to FCC-ee, match its sensitivity reach at high mass. For example, the new physics scale Λ, defined by the dimension-six operator $\hat{W} = 1/\Lambda^2\,(D_\rho W^a_{\mu\nu})^2$, will be constrained by the measurement of high-mass lepton pairs to $\Lambda > 80$ TeV. High-energy scattering of gauge bosons, furthermore, is a complementary probe of EW interactions at short distances. FCC-eh, with precision and energy in between those of FCC-ee and FCC-hh, will

Table 3 Measurement of selected electroweak quantities at the FCC-ee, compared with the present precision (1)

Observable	Present value ± error	FCC-ee stat.	FCC-ee syst.[a]	Comments and dominant experimental error
m_Z (keV/c^2)	91,186,700 ± 2,200	5	100	From Z line-shape scan, beam energy calibration
Γ_Z (keV)	2,495,200 ± 2,300	8	100	From Z line-shape scan, beam energy calibration
R_ℓ^Z ($\times 10^3$)	20,767 ± 25	0.06	0.2–1	Ratio of hadrons to leptons, acceptance for leptons
$\alpha_s(m_Z)$ ($\times 10^4$)	1,196 ± 30	0.1	0.4–1.6	From R_ℓ^Z above
R_b ($\times 10^6$)	216,290 ± 660	0.3	<60	Ratio of $b\bar{b}$ to hadrons, stat. extrapolation from SLD
σ_{had}^0 ($\times 10^3$) (nb)	41,541 ± 37	0.1	4	Peak hadronic cross-section, luminosity measurement
N_ν ($\times 10^3$)	2,991 ± 7	0.005	1	Z peak cross sections, luminosity measurement
$\sin^2\theta_W^{\text{eff}}$ ($\times 10^6$)	231,480 ± 160	3	2–5	From $A_{\text{FB}}^{\mu\mu}$ at Z peak, beam energy calibration
$1/\alpha_{\text{QED}}(m_Z)$ ($\times 10^3$)	128,952 ± 14	4	Small	From $A_{\text{FB}}^{\mu\mu}$ off peak
$A_{\text{FB}}^b, 0$ ($\times 10^4$)	992 ± 16	0.02	1–3	b quark asymmetry at Z pole, from jet charge
$A_{\text{FB}}^{\text{pol},\tau}$ ($\times 10^4$)	1,498 ± 49	0.15	<2	τ polarization and charge asymmetry, τ decay physics
m_W (keV/c^2)	80,350,000 ± 15,000	600	300	From WW threshold scan, beam energy calibration
Γ_W (keV)	2,085,000 ± 42,000	1,500	300	From WW threshold scan, beam energy calibration
$\alpha_s(m_W)$ ($\times 10^4$)	1,170 ± 420	3	Small	From R_ℓ^W
N_ν ($\times 10^3$)	2,920 ± 50	0.8	Small	Ratio of invisible to leptonic in radiative Z returns
m_{top} (MeV/c^2)	172,740 ± 500	20	Small	From $t\bar{t}$ threshold scan; QCD errors dominate
Γ_{top} (MeV)	1,410 ± 190	40	Small	From $t\bar{t}$ threshold scan; QCD errors dominate
$\lambda_{\text{top}}/\lambda_{\text{top}}^{\text{SM}}$	1.2 ± 0.3	0.08	Small	From $t\bar{t}$ threshold scan; QCD errors dominate
ttZ couplings	± 30%	<2%	Small	From E_{CM} = 365 GeV run

[a]The systematic uncertainties are present estimates and might improve with further examination. This set of measurements, together with those of the Higgs properties, will achieve indirect sensitivity to new physics up to a scale Λ of 70 TeV in a description with dimension-six operators, and possibly much higher in some specific new physics models.

Abbreviations: FCC-ee, Future Circular Collider electron–positron collider; SLD, SLAC Linear Collider Detector.

provide additional opportunities. For example, its ability to separate individual light-quark flavors in the proton will give it the best sensitivity to their EW couplings. Furthermore, its high energy and clean environment will enable precision measurements of the weak coupling evolution at very large Q^2. More details can be found in Reference 1.

EW measurements are a powerful element of the FCC discovery potential. They are also a crucial component of and a perfect complement to the FCC Higgs physics program.

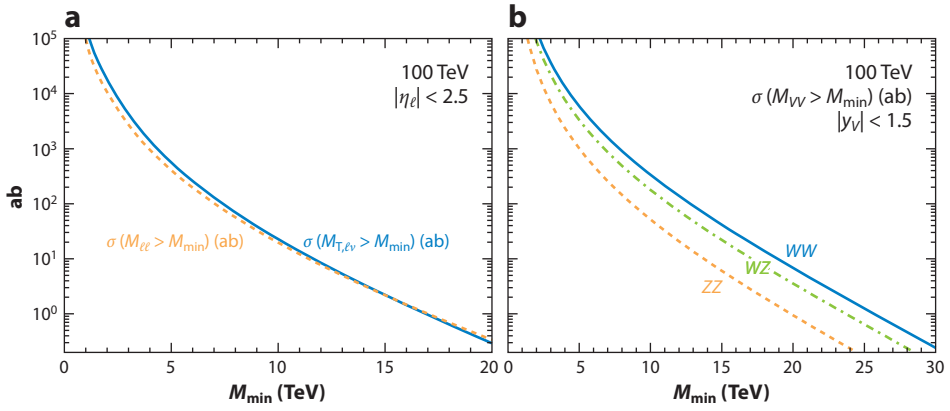

Figure 2

(*a*) Integrated lepton transverse (dilepton) mass distribution in $pp \to W^* \to \ell\nu$ ($pp \to Z^*/\gamma^* \to \ell^+\ell^-$) (1). One lepton family is included, with $|\eta_\ell| < 2.5$. (*b*) Integrated invariant mass spectrum for the production of gauge boson pairs in the central kinematic range $|y| < 1.5$ (1). No branching ratios are included.

2.3. The Electroweak Phase Transition

The challenge of explaining the origin of the cosmic matter–antimatter asymmetry is at the forefront of particle physics. One of the most compelling explanations connects this asymmetry to the generation of elementary particle masses through EWSB. This scenario relies on two ingredients: a sufficiently violent transition to the broken symmetry phase and the existence of adequate sources of *CP* violation. As it turns out, these conditions are not satisfied in the SM, but they can be met in a variety of beyond the Standard Model (BSM) scenarios. *CP* violation relevant to the matter–antimatter asymmetry can arise from new interactions over a broad range of mass scales, possibly well above 100 TeV. Exhaustively testing these scenarios may, therefore, go beyond the scope of the FCC. In contrast, for the phase transition to be sufficiently strong, there must be new particles with masses typically below 1 TeV whose interactions with the Higgs boson modify the Higgs potential energy in the early Universe. Should they exist, these particles and interactions would manifest at FCC, creating a key scientific opportunity and priority for the FCC, as shown by various studies completed to date (for a review, see Reference 1).

As an example, we show in **Figure 3** the results of the study of the extension of the SM scalar sector with a single real singlet scalar. The set of model parameters leading to a strong first-order phase transition is analyzed from the perspective of a direct search, via the decays of the new singlet scalar to a pair of Higgs bosons, and of precision measurements of Higgs properties. The former case is depicted in **Figure 3*a***. FCC-hh with 30 ab^{-1} has a sensitivity greater than 5σ to all relevant model parameters. For these models, the deviations in the Higgs self-coupling and in the Higgs coupling to the *Z* boson are depicted in **Figure 3*b***. With the exception of a small parameter range, most of these models lead to deviations within the sensitivity reach of FCC, which will allow cross-correlation of the direct discovery via di-Higgs decays to the Higgs property measurements. The cross-correlation will aid in the interpretation of a possible discovery and assess its relevance for the nature of the EW phase transition.

Matter–antimatter asymmetry: in the observable Universe, all galaxies are made from matter; this imbalance between matter and antimatter cannot be explained by the SM

2.4. Dark Matter

No experiment, at colliders or elsewhere, can probe the full range of DM masses allowed by astrophysical observations. However, there is a very broad class of models for which theory motivates

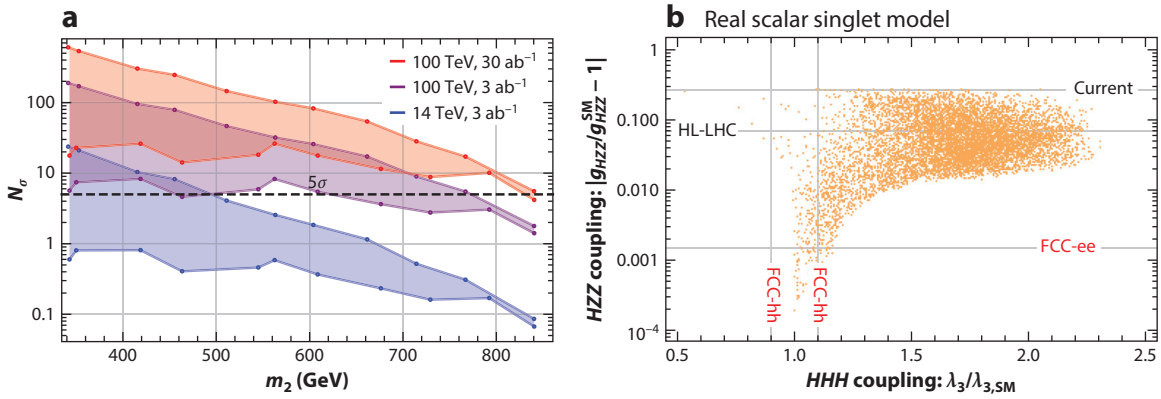

Figure 3

Manifestations of models with a singlet-induced strong first-order electroweak phase transition (1). (*a*) Discovery potential at the HL-LHC and FCC-hh for the resonant di-Higgs production as a function of the singlet-like scalar mass m_2. $\tau\tau\tau\tau$ and $b\bar{b}\gamma\gamma$ final states are combined. (*b*) Correlation between changes in the *HZZ* coupling (*vertical axis*) and the *HHH* coupling scaled to its Standard Model value (*horizontal axis*) in a scan of the model's parameter space. All points give rise to a first-order phase transition. Abbreviations: FCC, Future Circular Collider; FCC-ee, FCC electron–positron collider; FCC-hh, FCC hadron collider; HL-LHC, High-Luminosity Large Hadron Collider.

the GeV–tens of TeV mass scale, and that therefore could be in the range of the FCC. These are the models of WIMPs, which are present during the early Universe in thermal equilibrium with the SM particles. These conditions, broadly satisfied by many models of new physics, establish a correlation between the WIMP masses and the strength of their interactions, resulting in mass upper limits. While the absolute upper limit imposed by unitarity is around 110 TeV, most well-motivated models of WIMP DM do not saturate this bound but rather have upper limits on the DM mass in the TeV range. For example, DM WIMP candidates transforming as a doublet or triplet under the SU(2) group of weak interactions, such as the higgsinos and winos of supersymmetric theories, have masses constrained below ∼1 and ∼3 TeV, respectively. The full energy and statistics of FCC-hh will be necessary to access these large masses. With these masses, neutral and charged components of the multiplets are almost degenerate due to SU(2) symmetry, with calculable mass splittings induced by electromagnetic effects, in the range of a few hundred MeV. The peculiar signatures of these states are disappearing tracks left by the decay of the charged partner to the DM candidate and a soft, unmeasured charged pion. Dedicated analyses, including detailed modeling of various tracker configurations and realistic pileup scenarios, are described in Reference 1. **Figure 4** shows the results.

2.5. Direct Searches for New Physics

At the upper end of the mass range, the reach for the direct observation of new particles will be driven by the FCC-hh. The extension with respect to the LHC will scale as the energy increases, specifically, by a factor of five to seven, depending on the process. The detector parameters have been selected to guarantee the necessary performance up to the highest particle momenta and jet energies required for discovery of new particles with masses up to several tens of TeV. **Figure 5** shows examples of the discovery reach for the production of several types of new particles, as obtained by dedicated detector simulation studies. They include Z' gauge bosons carrying new weak forces and decaying to various SM particles, excited quarks Q^*, and massive gravitons G_{RS} present

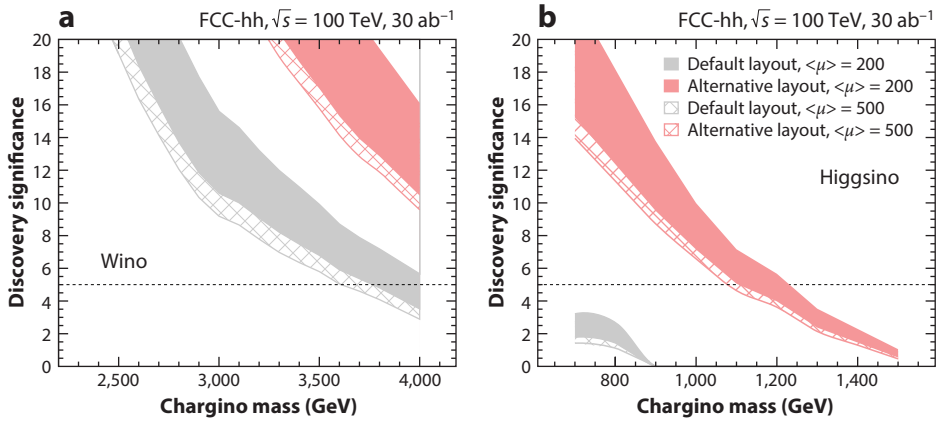

Figure 4

Expected discovery significance for (*a*) wino and (*b*) higgsino dark matter candidates at FCC-hh, with 500 pileup collisions (1). The gray and pink bands represent the significance using different layouts for the pixel tracker, as discussed in Reference 3. The width of the bands represents the difference between two models for the soft QCD processes. Abbreviations: FCC, Future Circular Collider; FCC-hh, FCC hadron collider.

in theories with extra dimensions. Other standard scenarios for new physics, such as supersymmetry (SUSY) or composite Higgs models, will likewise see the high-mass discovery reach greatly increased. The top scalar partners will be discovered up to masses of close to 10 TeV, gluinos up to masses of 20 TeV, and vector resonances in composite Higgs models up to masses close to 40 TeV. The direct discovery potential of FCC is not confined to the highest masses. In addition

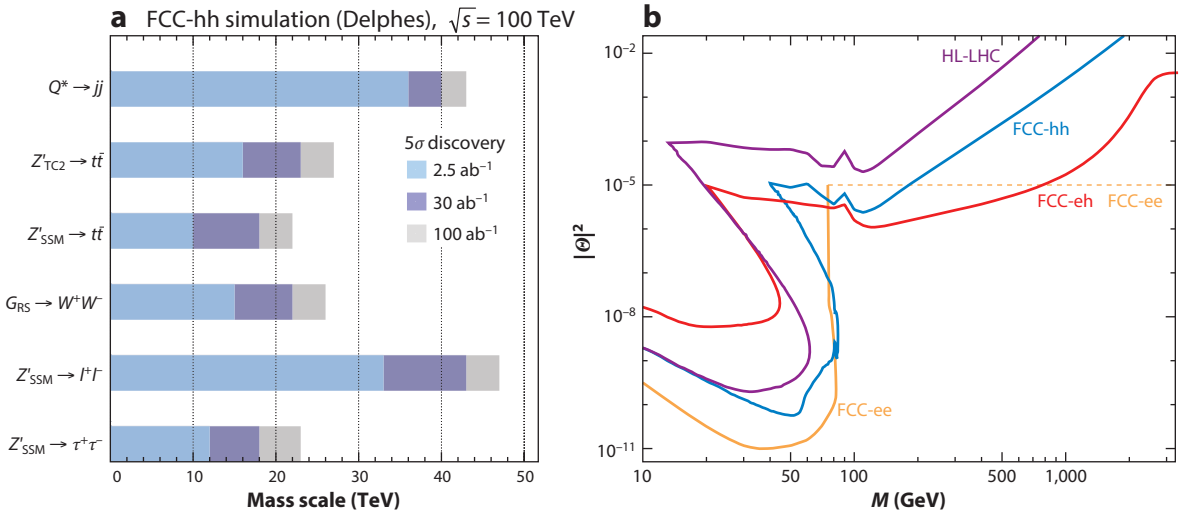

Figure 5

(*a*) FCC-hh mass reach for different s-channel resonances (1). (*b*) Summary of heavy sterile neutrino discovery prospects at all FCC facilities (1). The solid lines represent direct searches at FCC-ee (gold for Z decays), FCC-hh (blue for W decays), and FCC-eh (in production from the incoming electron). The dashed line denotes the impact on precision measurements at the FCC-ee; it extends up to more than 60 TeV. Abbreviations: FCC, Future Circular Collider; FCC-ee, FCC electron–positron collider; FCC-eh, FCC electron–proton collider; FCC-hh, FCC hadron collider; HL-LHC, High-Luminosity Large Hadron Collider.

to describing the DM examples presented above, Reference 1 documents the broad, and in most cases unique, reach for less-than-weakly-coupled particles, ranging from heavy sterile neutrinos (**Figure 5*b***) to the seesaw limit in a part of parameter space favorable for generating the baryon asymmetry of the Universe, as well as to axions and dark photons.

Supersymmetry (SUSY): relates bosons, which have integer spin, and fermions, which have half-integer spin; SUSY would solve many open problems in particle physics, but it predicts numerous supersymmetric partner particles, none of which has yet been observed

2.6. QCD Matter at High Density and Temperature

The thermodynamic behavior of QCD presents features that are unique among all other interactions. Heavy ions accelerated at FCC energies will provide access to an uncharted parton kinematic region at values of x down to 10^{-6}, which can be explored with the complementarity of proton–nucleus and electron–nucleus collisions at FCC-hh and FCC-eh. The quark–gluon plasma (QGP) could reach a temperature as high as 1 GeV, at which c quarks start to contribute as active thermal degrees of freedom in the equation of state of the QGP. In studies of the QGP with hard probes, the FCC has a unique edge thanks to cross-section increases with respect to the LHC by factors ranging from ∼20 for Z+jet production to ∼80 for top quark production. For example, the FCC will provide high rates of highly boosted top quarks, and the $q\bar{q}$ jets from $t \to W \to q\bar{q}$ will be exposed to energy loss in the QGP with a time delay (**Figure 6*a***), which will provide access to time-dependent density measurements for the first time. The effect of this time-delayed quenching can be measured using the reduction of the reconstructed W boson mass, as shown in **Figure 6*b***, which presents the modifications under different energy loss scenarios as examples.

2.7. Parton Structure

Deep-inelastic scattering measurements at FCC-eh will allow determination of PDF luminosities with high precision (1). These results will also provide an important input to the FCC-hh program of precision measurements and improve the sensitivity of the searches for new phenomena,

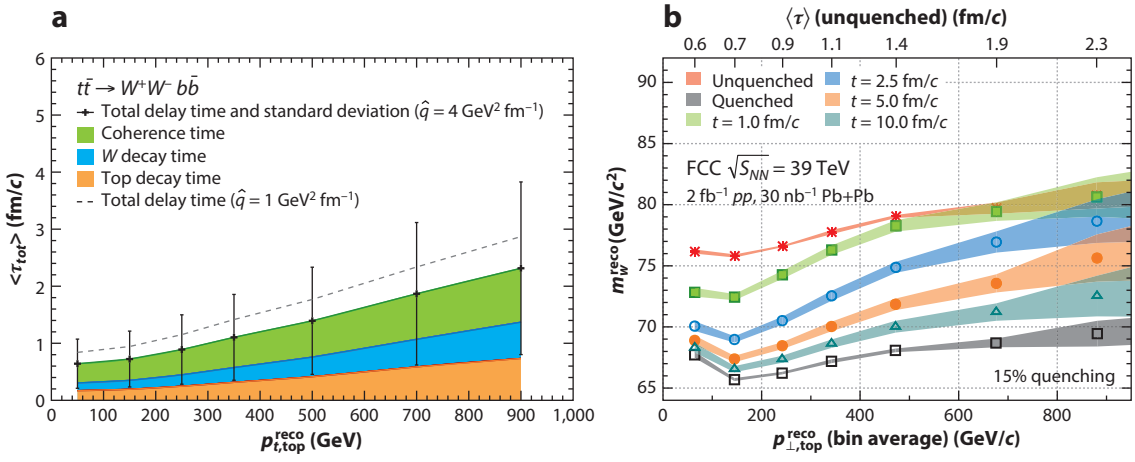

Figure 6

(*a*) Total delay time for the quark–gluon plasma energy-loss parameter $\hat{q} = 4$ GeV^2 fm^{-1} as a function of the top quark transverse momentum (*black dots*) and its standard deviation (*error bars*) (1). The average contribution of each component is shown as a colored stack band. The dashed line corresponds to $\hat{q} = 1$ GeV^2 fm^{-1}. (*b*) Reconstructed W boson mass as a function of the top quark p_T (1). The upper axis refers to the average total time delay of the corresponding top quark p_T bin. Abbreviation: FCC, Future Circular Collider.

Table 4 Expected production yields for *b*-flavored particles at FCC-ee at the *Z* run and at Belle II (50 ab^{-1}) for comparison (1, 5)

Particle production (10^9)	$B^0/\bar{B}^0$	B^+/B^-	$B_s^0/\bar{B}_s^0$	$\Lambda_b/\bar{\Lambda}_b$	$c\bar{c}$	$\tau^+\tau^-$
Belle II	27.5	27.5	NA	NA	65	45
FCC-ee	1,000	1,000	250	250	550	170

Abbreviation: FCC-ee, Future Circular Collider electron–positron collider.

particularly at high mass. FCC-eh measurements will extend the exploration of parton dynamics into previously unexplored domains: Access to very low Bjorken x is expected to expose the long-predicted BFKL (Balitsky–Fadin–Kuraev–Lipatov) dynamic behavior and the gluon saturation phenomena required to unitarize the high-energy cross sections. Determination of the gluon luminosity at very low x will also connect directly to ultrahigh-energy neutrino astroparticle physics, enabling more reliable estimates of the relevant background rates.

2.8. Flavor Physics

The FCC flavor program will receive important contributions from all three machines, FCC-ee, FCC-hh, and FCC-eh. The FCC-ee Z run will record, with no trigger, 10^{12} $Z \to b\bar{b}$ and $Z \to c\bar{c}$ events. This run will yield high statistics of all b- and c-flavored hadrons, making FCC-ee the natural continuation of the B factories (**Table 4**).

Of topical interest will be the study of possible lepton-flavor and lepton-number violation. FCC-ee, with detection efficiencies internally mapped with extreme precision, will offer 200,000 $B_0 \to K^*(892)e^+e^-$, 1,000 $K^*(892)\tau^+\tau^-$, and 1,000 (100) B_s (B_0) events, one order of magnitude more than the LHCb upgrade. The determination of the Cabibbo–Kobayashi–Maskawa parameters will correspondingly improve. The first observation of CP violation in B mixing will be within reach; a global analysis of BSM contributions in box mixing processes, assuming minimal flavor violation, will provide another, independent, test of BSM physics up to an energy scale of 20 TeV.

τ physics in Z boson decays has already been shown to be extremely precise at LEP. With 1.7×10^{11} pairs, FCC-ee will achieve a precision of 10^{-5} or better for the leptonic branching ratios and the charged lepton–neutrino weak couplings, which will allow measurement of G_F and tests of charged-weak-current universality at the 10^{-5} precision level. Finally, lepton-number-violating processes, such as $Z \to \tau X$ ($X = \mu, e$) or $\tau \to \mu\mu\mu, e\gamma$, or $\mu\gamma$, could be detected at the 10^{-9}–10^{-10} level, offering sensitivity to several types of new physics, in particular neutrino mass–generation models.

3. THE LEPTON COLLIDER (FCC-ee)

The FCC-ee accelerator design provides high luminosity at two (or more) experiments for several different collision energies between 90 and 365 GeV, while satisfying several stringent optics constraints (6). Apart from a ±1.2-km-long section around each interaction point (IP), the machine follows the layout of the 97.75-km-circumference hadron collider, FCC-hh (see Section 4). The present design foresees two IPs. The synchrotron radiation power is limited to 50 MW per beam at all energies.

3.1. Machine Design and Layout

For a collision energy of 365 GeV, as required for $t\bar{t}$ operation, the cost-optimized circumference is approximately 100 km (7). FCC-ee is designed as a double-ring collider, such as the KEKB and

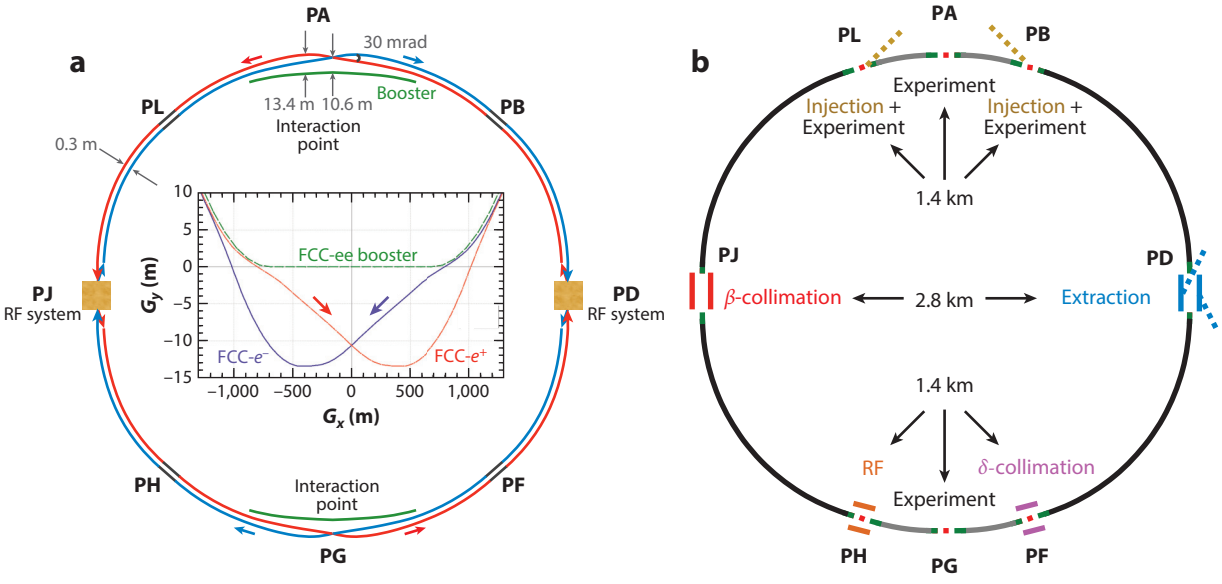

Figure 7

Overall layout of the two FCC colliders housed successively in the same tunnel. (*a*) FCC-ee layout with a zoomed-in view of the trajectories across IP PG (2). The FCC-ee rings are placed 1 m outside the FCC-hh footprint in the arc. The main booster follows the footprint of the FCC-hh. In the arc, the e^+ and e^- rings are horizontally separated by 30 cm. The IPs are shifted by 10.6 m toward the outside of FCC-hh. The beam trajectories toward each IP are straighter than the outgoing ones in order to reduce the synchrotron radiation at the IP (10). (*b*) FCC-hh layout, indicating the main insertions (3). The experiment IPs are at PA, PB, PG, and PL. Injection takes place at PL and PB. PD hosts the beam extraction. Collimation takes place at PF and PJ. The RF systems are installed at PH. Abbreviations: FCC, Future Circular Collider; FCC-ee, FCC electron–positron collider; FCC-hh, FCC hadron collider; IP, interaction point; RF, radio-frequency.

PEP-II *B* factories. The double-ring configuration (**Figure 7*a***) allows a large number of bunches. The two beam lines cross at two IPs with a horizontal crossing angle of 30 mrad. A crab waist collision scheme (8, 9) that profits from the crossing angle has been adopted, enabling an extremely small vertical β function β_y^* at the IP (about 50 times smaller than at LEP) and a high beam–beam tune shift. This novel collision scheme has been successfully used at DAΦNE since 2008–2009. The critical energy of the synchrotron radiation of the incoming beams toward the IPs is kept below 100 keV at all beam energies (6, 10). A common lattice is used for all beam energies, except for a small rearrangement in the radio-frequency (RF) section for the $t\bar{t}$ mode. The betatron tune, phase advance in the arc cell, final focus optics, and configuration of the sextupoles are set to the optimum at each energy by changing the strengths of the magnets. The two experiments are situated in points PA and PG. The length of the free area around the IP (ℓ^*) and the strength of the detector solenoid are kept constant at 2.2 m and 2 T, respectively, for all energies. A so-called tapering scheme scales the strengths of all magnets, apart from the solenoids, according to the local beam energy, taking into account the energy loss due to synchrotron radiation. Two RF sections per ring are placed in the straight sections at points PD and PJ. The RF cavities are common to e^+ and e^- in the case of $t\bar{t}$.

3.2. Parameters

Table 5 presents the FCC-ee machine parameters. The beam current varies greatly between the Z pole and the $t\bar{t}$ threshold. The current is adjusted by changing the number of bunches. In existing

Table 5 Machine parameters of the FCC-ee for different beam energies (2)

	Z	*WW*	*ZH*	$t\bar{t}$[a]	
Circumference (km)			97.756		
Bending radius (km)			10.76		
Free length to IP l^* (m)			2.2		
Solenoid field at IP (T)			2		
Full crossing angle at IP, θ (mrad)			30		
SR power per beam (MW)			50		
Beam energy (GeV)	45.6	80	120	175	182.5
Beam current (mA)	1,390	147	29	6.4	5.4
Bunches per beam	16,640	2,000	328	59	48
Average bunch spacing (ns)	19.6	163	994	2,763	3,396
Bunch population (10^{11})	1.7	1.5	1.8	2.2	2.3
Horizontal emittance, ε_x (nm)	0.27	0.84	0.63	1.34	1.46
Vertical emittance, ε_y (pm)	1.0	1.7	1.3	2.7	2.9
Horizontal β_x^* (m)	0.15	0.2	0.3	1.0	
Vertical β_y^* (mm)	0.8	1.0	1.0	1.6	
Energy spread in collision, σ_δ (%)	0.132	0.131	0.165	0.186	0.192
Bunch length in collision, σ_z (mm)	12.1	6.0	5.3	2.62	2.54
Piwinski angle (SR/BS), ϕ	8.2/28.5	3.5/7.0	3.4/5.8	0.8/1.1	0.8/1.0
Energy loss per turn (GeV)	0.036	0.34	1.72	7.8	9.2
RF frequency (MHz)		400		400/800	
RF voltage (GV)	0.1	0.75	2.0	4.0/5.4	4.0/6.9
Longitudinal damping time (turns)	1,273	236	70.3	23.1	20.4
Energy acceptance (DA) (%)	±1.3	±1.3	±1.7	−2.8, +2.4	
Polarization time t_p (min)	15,000	900	120	18.0	14.6
Luminosity per IP (10^{34} cm^{-2} s^{-1})	230	28	8.5	1.8	1.55
Vertical beam–beam parameter, ξ_y	0.133	0.113	0.118	0.128	0.126
Beam lifetime (min)	>200	>200	18	24	18

[a]A common RF system is used for $t\bar{t}$ operation. Abbreviations: BS, beamstrahlung; DA, dynamic aperture; FCC-ee, Future Circular Collider electron–positron collider; IP, interaction point; RF, radio-frequency; SR, synchrotron radiation.

electron-storage rings, the equilibrium beam parameters are determined by synchrotron radiation generated in the dipoles of the collider arcs. For FCC-ee, the energy spread and the beam lifetime are also affected by beamstrahlung, which is a special type of synchrotron radiation, emitted during the collision due to the field of the opposite bunch. The bunch population varies slightly and is chosen for maximum luminosity at each energy, taking into account the effect of beamstrahlung.

3.3. Injection

A top-up injection scheme (11) maintains the stored beam current and the luminosity at the highest level throughout the physics run. Without top-up injection, the integrated luminosity would be more than an order of magnitude lower. Therefore, it is necessary to install a booster synchrotron in the collider tunnel.

Injection into the top-up booster takes place at 20 GeV, similar to injection into LEP. The layout of the preinjector complex resembles that of the KEKB/SuperKEKB injector. For FCC-ee, it consists of a 6 GeV normal-conducting S-band linac, a prebooster (possibly the SPS) that accelerates the electron and positron beams from 6 to 20 GeV, a positron source where

4.46 GeV electrons from the linac are sent onto a hybrid target with flux concentrator, and a small positron damping ring. The linac will accelerate one or two bunches per pulse at a repetition rate of 100 or 200 Hz. The complete filling for Z running is the most demanding with respect to the number of bunches, bunch intensity, and, therefore, injector flux. It requires a linac bunch intensity of 2×10^{10} particles for both species. The required positron rate is similar to the rates at SuperKEKB and the SLC. Alternative injector scenarios include a longer 20 GeV linac, without any prebooster.

3.4. Performance

As a result of renewed worldwide interest in e^+e^- physics and its associated discovery potential since the observation of the Higgs boson at the LHC, the FCC-ee is not alone in its quest. At the time of writing this article, four separate e^+e^- collider designs have been suggested to study the properties of the Higgs boson and other SM particles with unprecedented precision. These include (*a*) the International Linear Collider (ILC) (12) project, with a center-of-mass energy of 250 GeV (13, 14); (*b*) the Compact Linear Collider (CLIC) (15), whose lowest center-of-mass energy point was reduced from 500 to 380 GeV (16); (*c*) the Circular Electron–Positron Collider (CEPC) (17–19), in a 100-km-long tunnel; and (*d*) FCC-ee [the Future e^+e^- Circular Collider, formerly called TLEP (20, 21)] in a new ∼100-km-long tunnel at CERN. **Figure 8** illustrates the baseline luminosities expected to be delivered at each of the four colliders.

Figure 9 depicts the expected integrated luminosities and operation phases at each energy. FCC-ee delivers the highest rates in a clean, well-defined, and precisely predictable environment, at the Z pole (91 GeV), at the WW threshold (161 GeV), as a Higgs factory (240 GeV), and around the $t\bar{t}$ threshold (350 to 365 GeV), to two IPs. Thanks to the availability of transverse polarization to a beam energy of up to 80 GeV or more (22), it also provides high-precision center-of-mass

International Linear Collider (ILC): a 250 GeV e^+e^- collider, proposed to be built in Japan, that is based on two superconducting L-band linacs, a technology that has been under development since the late 1980s for the TESLA project

Compact Linear Collider (CLIC): in its first stage, a proposed 380 GeV e^+e^- collider based on two warm X-band linacs, driven by two-beam acceleration. CLIC has been under development at CERN since the early 1980s

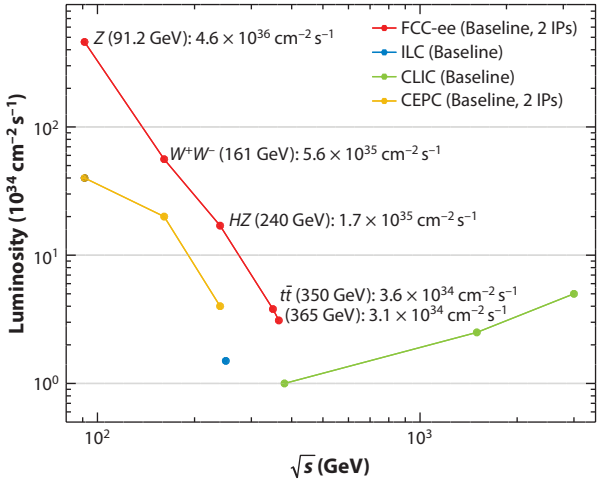

Figure 8

Baseline luminosities expected to be delivered (summed over all interaction points), as a function of the center-of-mass energy $\sqrt{s}$, at each of the four worldwide e^+e^- collider projects: ILC (*blue circles*), CLIC (*green circles*), CEPC (*gold circles*), and FCC-ee (*red circles*). FCC-ee performance data are from Reference 2, the latest incarnation of the CEPC parameters is inferred from Reference 19, and the linear collider luminosities are from References 14 and 16. Abbreviations: CEPC, Circular Electron–Positron Collider; CLIC, Compact Linear Collider; FCC, Future Circular Collider; FCC-ee, FCC electron–positron collider; ILC, International Linear Collider; IP, interaction point.

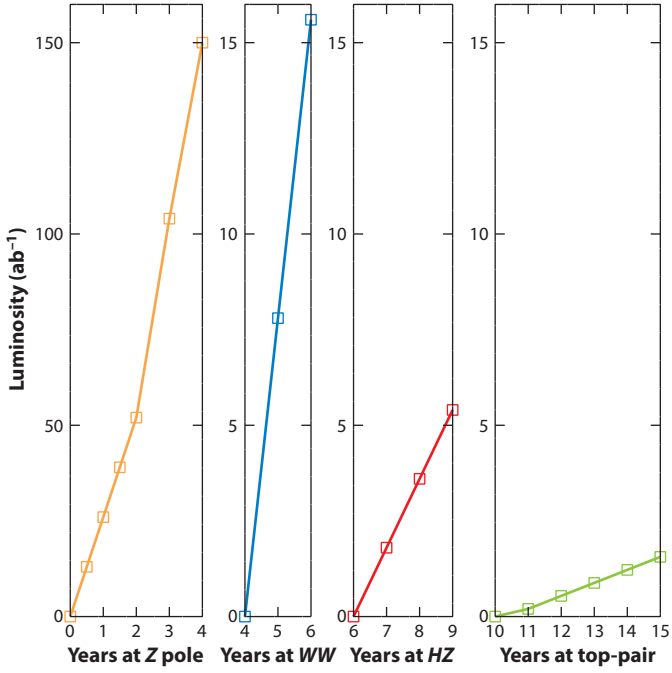

Figure 9

Operation model for FCC-ee (2), showing the integrated luminosity at the Z pole (*gold*), the WW threshold (*blue*), the Higgs factory (*red*), and the top-pair threshold (*green*) as a function of time. The gap between years 9 and 10 reflects the shutdown time needed to prepare the collider for the highest-energy runs. Abbreviation: FCC-ee, Future Circular Collider electron–positron collider.

energy calibration at the 100 keV level at the Z and W energies (23; see also **https://indico.cern.ch/event/669194**), a unique feature of circular colliders. FCC-ee, therefore, is genuinely best suited to offer extreme statistical precision and experimental accuracy for the measurement of the SM particle properties, opens a windows to the detection of new rare processes, and furnishes opportunities to observe tiny violations of established symmetries.

Circular Electron–Positron Collider (CEPC): a 91–240 GeV e^+e^- collider, with a circumference of 100 km, proposed to be built in China. A Super Proton–Proton Collider (SPPC), with a collision energy of 75–125 TeV, could later share the same tunnel

3.5. Technical Systems

Table 5 shows that the FCC-ee machine faces quite different requirements in its various modes of operation. For example, on the Z pole, FCC-ee is an ampere-class storage ring, similar to PEP-II, KEKB, and DAΦNE, with a high beam current but a low RF voltage, of order 0.1 GV. For the $t\bar{t}$ mode, the beam current is only a few milliamperes, as for the former LEP2, while an RF voltage above 10 GV is required. In both cases, a total of 100 MW RF power must be constantly supplied to the two circulating beams.

Three sets of superconducting RF cavities are proposed to cover all operation modes for the FCC-ee collider rings and booster:

1. for high-intensity operation (Z, FCC-hh), 400 MHz monocell cavities (four per cryomodule), based on niobium/copper thin-film technology at 4.5 K;
2. for higher-energy operation (W, H, $t\bar{t}$), 400 MHz four-cell cavities (four per cryomodule), again based on niobium/copper technology at 4.5 K; and

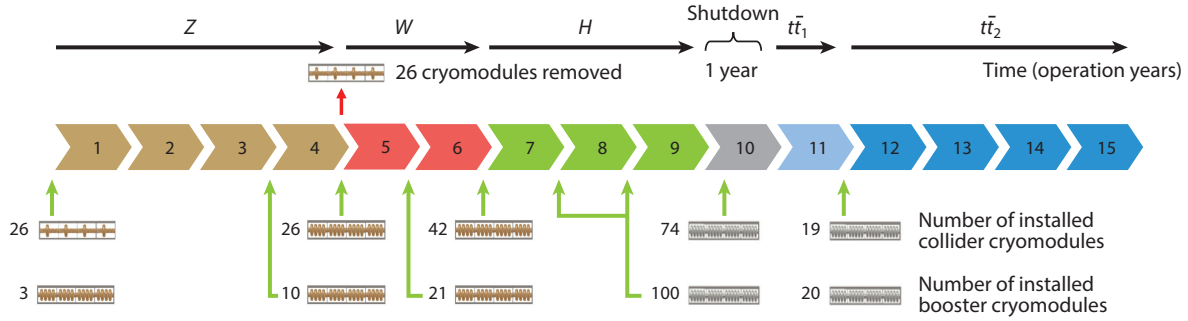

Figure 10

Operation timeline for FCC-ee (2). (*Bottom*) The number of cryomodules to be installed in the collider and booster, respectively, during the various winter shutdown periods (also see Reference 26). Abbreviation: FCC-ee, Future Circular Collider electron–positron collider.

3. for the $t\bar{t}$ machine, a complement of 800 MHz five-cell cavities (again, four per cryomodule), based on bulk niobium at 2 K.

The installation sequence (**Figure 10**) is comparable to that of LEP, where approximately 30 cryomodules were installed per shutdown. The FCC-ee superconducting RF cavities may require kilowatt-range superfluid-helium refrigeration operating down to 1.6 K. Magnetic refrigeration operating below 4.2 K is being studied as an alternative to compression/expansion helium refrigeration (24). The proposed staged RF system will result in acceptable levels of higher-order-mode power per cavity, provided that the bunch-filling patterns are properly chosen (25).

The accelerator impedance is dominated by the resistive wall of the vacuum chamber, driving coupled-bunch motion, which can be cured by a feedback system, as well as the single-bunch microwave instability of the short bunches (27). For FCC-ee, a novel ultrathin nonevaporable getter coating for the vacuum chamber has been developed; it does not degrade the effective impedance but still efficiently reduces the secondary emission yield, thereby suppressing the buildup of an electron cloud (28). High overall energy efficiency is achieved through a combination of different technical and operational measures, for example, by using advanced RF power sources (29), novel low-power twin-aperture magnets (30), and top-up injection.

4. THE HADRON COLLIDER (FCC-hh)

The combined data sets from the two FCC-hh experiments will significantly exceed the total of 30 ab^{-1} required by the planned physics studies. In addition, FCC-hh will offer the potential to collide ions with protons and ions with ions (31). The design allows for the upgrade of one IP to electron–proton and electron–ion collisions. In that case, an additional recirculating, energy-recovery linac will provide the electron beam that collides with one circulating proton or ion beam. The other experiments could operate with hadron collisions concurrently.

Nonevaporable getters: mostly porous alloys of aluminum, zirconium, titanium, vanadium, and iron for ultrahigh vacuums and with low secondary electron emission yield

4.1. Layout and Design

Figure 7*b* shows the layout of the collider, and **Table 6** presents the key parameters. The circumference of the collider is 97.75 km, and the insertions are 1.4 km long, with the exception of the 2.8-km-long transverse collimation and beam extraction areas. This additional length facilitates

Table 6 Key FCC-hh baseline parameters compared with LHC and HL-LHC parameters (3)

	LHC	HL-LHC	FCC-hh	
			Initial	Nominal
Physics performance				
Peak luminosity[a] (10^{34} cm^{-2} s^{-1})	1.0	5.0	5.0	<30.0
Optimum average integrated luminosity per day (fb^{-1})	0.47	2.8	2.2	8
Assumed average turnaround time (h)	5	4	5	4
Peak number of inelastic events per crossing	27	135 leveled	171	1,026
Total/inelastic cross section σ proton (mb)	111/85		153/108	
Luminous region RMS length (cm)	4.5	4.0	5.3	4.9
Distance from IP to first quadrupole, ℓ^* (m)	23	40	40	
Beam parameters				
Number of bunches, n	2,808		10,400	
Bunch spacing (ns)	25			
Bunch population, N (10^{11})	1.15	2.2	1.0	
Nominal transverse normalized emittance (μm)	3.75	2.5	2.2	2.2
Number of IPs contributing to ΔQ	3	2	2+2	2
Maximum total beam–beam tune shift, ΔQ	0.01	0.015	0.011	0.03
Beam current (A)	0.584	1.12	0.5	
RMS bunch length[b] (cm)	7.55		8	
IP β function (m)	0.55	0.15 (min)	1.1	0.3
RMS IP spot size (μm)	16.7	7.1 (min)	6.8	3.5
Full crossing angle (μrad)	285	590	104	200[c]

[a]For the nominal parameters, the peak luminosity will be reached during the run.
[b]The HL-LHC assumes a different longitudinal distribution; the equivalent Gaussian is 9 cm.
[c]The crossing angle will be compensated for using the crab crossing scheme.
Abbreviations: FCC-hh, Future Circular Collider hadron collider; HL-LHC, High-Luminosity LHC; IP, interaction point; LHC, Large Hadron Collider; RMS, root mean square.

the mitigation of the technological challenges generated by the high beam energies. An integrated lattice includes all the required functions.

Two high-luminosity experiments are located in opposite insertions (PA and PG), which ensures the highest luminosity, reduces unwanted beam–beam effects, and is independent of the beam-filling pattern. The main experiments are located in 66-m-long halls, sufficient for the detector design discussed here. The final-focus system has been integrated into the available length of the insertion. The detector magnet systems may be constructed without any iron (32). Two additional, lower-luminosity experiments, together with the injection systems, are located in insertions PB and PL. In contrast to the LHC, these experiments are not located in the center of their insertions, to allow more space for the injection region and better protection of the experiments from the injected beam. The collider will use the existing CERN accelerator complex as its injector facility. The baseline injection concept is to inject the beam at 3.3 TeV from the LHC. Injection from a new, superconducting SPS could be considered as an alternative. The transverse beam cleaning is located in insertion PJ, and the beam extraction is in insertion PD. The longitudinal beam cleaning is located in insertion PF, and the RF systems and fast feedback are located in insertion PH. The long arcs also contain technical points (PC, PE, PI, and PK; not shown in **Figure 7**).

This layout increases the collider's robustness because the high-luminosity experiments and collimation sections are separated from the radiation-sensitive equipment, namely the RF, instrumentation, and extraction kickers. Also, the short arcs between the main experiment in PA and

the additional experiments in PB and PL are long enough to avoid background from the collision debris in the main experiment, which would perturb the other experiments. Similarly, the RF insertion is protected from the main experiment in PG.

Beamscreen: a coaxial liner that intercepts synchrotron radiation inside the cold arcs at a temperature significantly higher than the 1.9 K of the superconducting magnets, ensures optimum cooling efficiency, and minimizes dynamic vacuum effects

4.2. Injection

The baseline injection concept reuses CERN's Linac 4, PS, PSB, SPS, and the LHC at 3.3 TeV as preaccelerators and connects the LHC to FCC-hh with transfer lines using 7 T superconducting magnets. This choice also permits the continuation of CERN's rich and diverse fixed-target physics program in parallel with FCC-hh operation. The necessary modifications to the LHC are considered limited and feasible; in particular, the ramp speed can be increased as needed.

Reliability and availability studies have confirmed that operation can be optimized such that the FCC-hh collider will have adequate availability for luminosity production. However, the power consumption of the aging LHC cryogenic system poses a concern. The required 80–90% availability of the injector chain could best be achieved with a new high-energy booster. As an alternative, direct injection from a new superconducting synchrotron at 1.3 TeV that would replace the current 6.7-km-long SPS could be considered. In that case, simpler normal conducting transfer lines with magnets operating at 1.8 T would be sufficient. For this scenario, additional studies of beam stability in the collider at injection would be required.

4.3. Energy Reach

The total length of the arcs is 83.75 km. The lattice in the arc consists of 90° phase advance regular focusing–defocusing (FODO) cells with a length of approximately 213 m and six 14-m-long dipoles between quadrupoles. The dipole filling factor is approximately 0.8; therefore, a dipole field just below 16 T is required to keep the nominal beams on the circular orbit.

The dipoles use Nb_3Sn conductors at a temperature of 2 K to reach this field and are a key cost item. A focused research and development (R&D) program to increase the maximum current density in the conductors to at least 1,500 A mm^{-2} at 4.2 K began in 2014 (1,200 A mm^{-2} has been achieved). On the basis of this performance, several optimized dipole designs have been developed by a the EuroCirCol H2020 project funded by the European Commission; each implements a different design concept. The development of different designs enabled comparative analysis (e.g., the amount of conductor required) and led to the choice of the $\cos\theta$ design as the baseline. Collaboration agreements are in place with the French Alternative Energies and Atomic Energy Commission; the Italian Institute of Nuclear Physics; the Spanish Centre for Energy, Environment and Technology; the Swiss Paul Scherrer Institute; and the Russian Budker Institute of Nuclear Physics to build short model magnets based on the designs. In addition, a US Department of Energy Magnet Development program is working to demonstrate a 15 T superconducting accelerator magnet. Quench protection systems for the FCC-hh 16 T dipoles are an integral part of the magnet design (33). A worldwide FCC-hh R&D program is developing superconducting wires and optimizing the high-field magnet designs.

If FCC-hh is implemented following a lepton collider (FCC-ee) in the same underground infrastructure, the timescale for design and R&D for FCC-hh would be lengthened by 15 to 20 years. This additional time would be used to develop alternative technologies, such as magnets based on high-temperature superconductors, which may have a significant impact on the collider parameters (e.g., increase of beam energy), relaxed infrastructure requirements (cryogenics system), and increased energy efficiency (temperature of magnets and beamscreen).

4.4. Luminosity Performance

It is anticipated that the initial parameters will be reached with a maximum luminosity of 5×10^{34} $cm^{-2}s^{-1}$ in the first years of operation. Thereafter, the luminosity will be increased to reach the nominal parameters with a luminosity of up to 3×10^{35} $cm^{-2}s^{-1}$. The estimated integrated luminosity is 2 fb^{-1} per day of operation for the initial parameters and 8 fb^{-1} per day for the nominal parameters. A generic design for the low-luminosity experiments shows that a luminosity of 2×10^{34} $cm^{-2}s^{-1}$ could be reached, but further studies are required.

The high luminosity is achieved with high-brightness beams, a high beam current comparable to LHC parameters, and a small β^* at the collision points. Crossing the beams at an angle limits the impact of parasitic beam–beam interactions. Crab cavities compensate for the associated luminosity reduction. Electron lenses and current-carrying wire compensators may further improve the performance of the machine.

In the nominal phase, the beams can only be used for approximately 3.5 h in collision due to the fast beam burn-off. Consequently, the turnaround time from one luminosity run to the next is critical to achieve the target integrated luminosity (34). Theoretically, a time of approximately 2 h can be achieved. However, to include sufficient margin, turnaround times of 5 h and 4 h are assumed for initial and nominal parameters, respectively. An availability of 70% for physics operation is assumed for the estimate of the overall integrated luminosity. The FCC-hh availability has been modeled on the basis of the LHC experience (35).

The various beam dynamics effects that can compromise beam stability and quality were investigated and modeled for the conceptual design; mitigation methods have been devised where required. A combination of fast transverse feedback and octupoles is used to stabilize the beam against parasitic electromagnetic interaction with the beamline components. Electron cloud buildup, which could render the beam unstable, is suppressed by appropriate hardware design. The impact of main magnet field imperfections on the beam is mitigated by high-quality magnet design and use of corrector magnets.

4.5. Technical Systems

Many technical systems and operational concepts for FCC-hh can be scaled up from the HL-LHC or can be based on technology demonstrations carried out in the frame of ongoing R&D projects. Particular technological challenges arise from the higher total energy in the beam (20 times that of the LHC), the much-increased collision debris in the experiments (40 times that of the HL-LHC), and far higher levels of synchrotron radiation in the arcs (200 times that of the LHC).

The high luminosity and beam energy will produce collision debris with a power of up to 0.5 MW in the main experiments (36). A significant fraction of this energy will be lost in the machine near the experiment. A sophisticated shielding system, similar to that of the HL-LHC but thicker, protects the final focusing triplet, avoids quenches, and reduces the radiation dose. The current radiation limit of 30 MGy for the magnets, resulting from the resin used, will be reached for an integrated luminosity of 13 ab^{-1}. However, improvement of both the shielding and the radiation hardness of the magnets appears possible. Therefore, it is likely that the magnets will not have to be replaced during the entire lifetime of the collider.

The robust collimation and beam extraction system protects the machine from the energy stored in the beam. The collimation system design is based on the LHC system, with a number of improvements to make it viable. Additional protection has been added to mitigate losses in the arcs, which would otherwise quench or even damage magnets (37). Also, improved

conceptual designs of collimators and dogleg dipoles have been developed to reduce beam-induced stress to acceptable levels. Further R&D should allow the margin in the design to be increased to comfortable levels.

The extraction system uses a segmented, dual-plane dilution kicker system to distribute all bunches of the beam in a multibranch spiral on the absorber block (38). Novel superconducting septa capable of deflecting the rigid beams are currently being developed (39). The system design is fault tolerant; in particular, the most critical failure mode—erratic firing of a single extraction kicker element—has limited impact since the system has high granularity. Investigations of suitable absorber materials, including three-dimensional carbon composites and carbon foams, are ongoing in the HL-LHC project.

The cryogenics system must compensate for the continuous heat loads in the arcs of 1.4 W m^{-1} at a temperature below 2 K and 30 W m^{-1} per aperture due to synchrotron radiation at a temperature of 50 K, as well as absorbing the transient loads from ramping of the magnets. The system must also be able to fill and cool down the cold mass of the machine (230×10^6 kg) in less than 20 days, while avoiding thermal gradients higher than 50 K in the cryomagnet structure. It must also cope with resistive transitions of the superconducting magnets and recover sufficiently quickly from such situations that the operational availability of the collider remains at an adequate level.

Today, helium cryogenic refrigeration reaches efficiencies of only ~30% with respect to an ideal Carnot cycle, leading to high electrical power consumption. Part of the FCC study is to perform R&D on novel concepts for refrigeration down to 40 K based on a neon–helium (nelium) gas mixture, which has the potential to reach efficiencies higher than 40%. This technology could reduce the electrical energy consumption of the cryogenics system by 20%.

The cryogenic beam vacuum system ensures excellent vacuum to limit beam-gas scattering. It also protects the magnets from the synchrotron radiation of the high-energy beam and efficiently removes the heat. In addition, it avoids beam instabilities due to parasitic beam–surface interactions and electron cloud effects. The LHC beamscreen design is not suitable for FCC-hh; therefore, a novel design has been developed in the scope of the EuroCirCol H2020 funded project. It is as compact as possible to minimize the magnet aperture and resulting magnet cost. The FCC-hh beamscreen features an antechamber and is copper coated to limit parasitic interaction with the beam. The shape also reduces seeding of the electron cloud by backscattered photons, and additional carbon coating or laser treatment prevents buildup. This novel system is operated at 50 K. A prototype has been experimentally validated in the KARA synchrotron radiation facility at KIT in Germany.

The RF system is similar to that of the LHC, with a frequency of 400 MHz, but provides a higher maximum total voltage of 48 MV. Controlled longitudinal emittance blow-up by band-limited RF phase noise is employed in order to adjust the bunch length in the presence of longitudinal damping by synchrotron radiation. The current design uses 24 single-cell cavities.

4.6. Ion Operation

A preliminary parameter set for ion operation has been developed on the basis of current injector performance. If two experiments operate simultaneously for 30 days, the expected integrated luminosity of each of them would be 6 pb^{-1} and 18 pb^{-1} for proton–lead ion operation with initial and nominal parameters, respectively. For lead ion operation, integrated luminosities of 23 nb^{-1} and 65 nb^{-1} could be expected. More detailed studies are being carried out to address the key issues in ion production and collimation and to review the luminosity predictions.

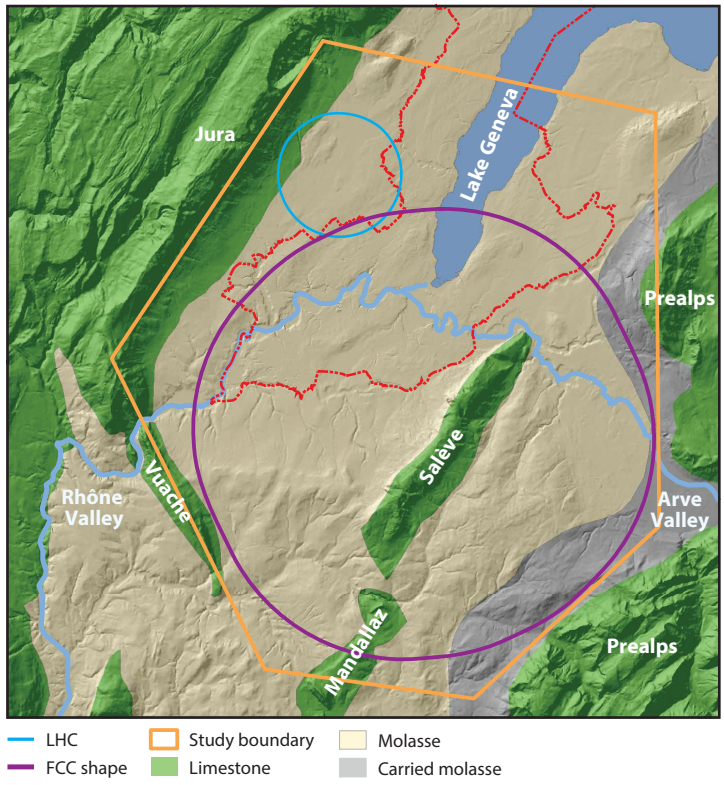

Figure 11

Study boundary (*orange polygon*) showing the main topographical and geological structures, Large Hadron Collider (LHC) (*blue circle*), and Future Circular Collider (FCC) tunnel trace (*purple circle*) (2).

5. INFRASTRUCTURE

Figure 11 presents the proposed location of the FCC. The principal structure of the FCC lepton and hadron colliders is a quasi-circular 97.75-km-long tunnel composed of arc segments interleaved with straight sections. The tunnel location and depth have been optimized by taking the local geology into account. Construction of this tunnel is feasible even in such a densely built area. The transverse tunnel diameter in the arcs is 5.5 m. Approximately 8 km of bypass tunnels, 18 shafts, 14 large caverns, and 12 new surface sites are also planned. **Figure 12** presents a cross section of the FCC tunnel in a typical arc segment, with integrated air-supply and smoke-extraction ducts.

6. TIMELINE

Implementation of the first stage, the intensity-frontier lepton collider FCC-ee, will commence with a preparatory phase of 8 years, followed by the construction phase (all civil and technical infrastructure, machines, and detectors, including commissioning) lasting 10 years. A duration of 15 years is projected for the subsequent operation of the FCC-ee facility, to complete the currently envisaged physics program. The total time for construction and operation of FCC-ee is nearly 35 years.

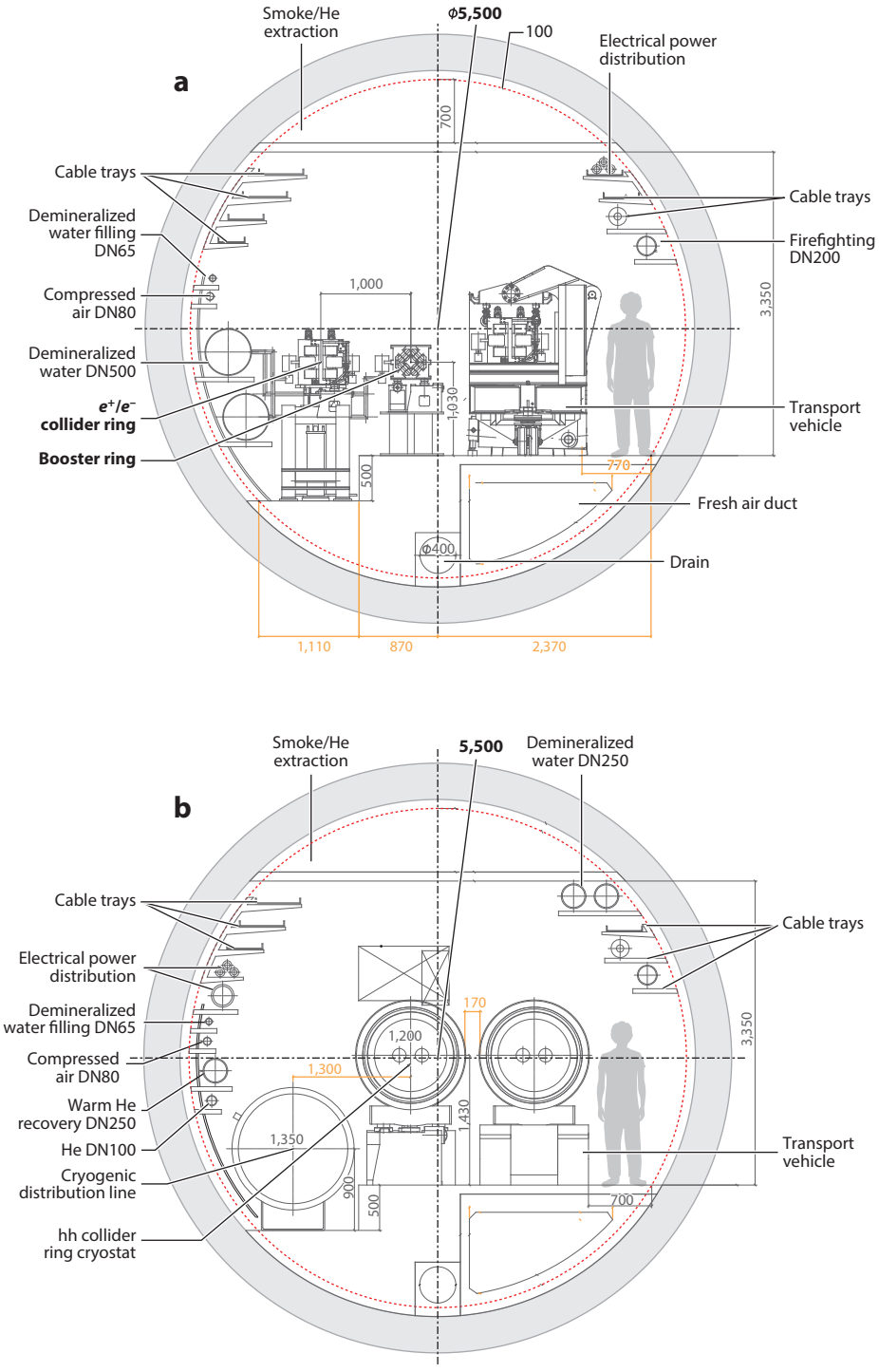

Figure 12

Machine tunnel cross section in a regular arc with machine elements, services, and transport equipment. (*a*) FCC electron–positron collider (2). (*b*) FCC hadron collider (3). Abbreviation: FCC, Future Circular Collider.

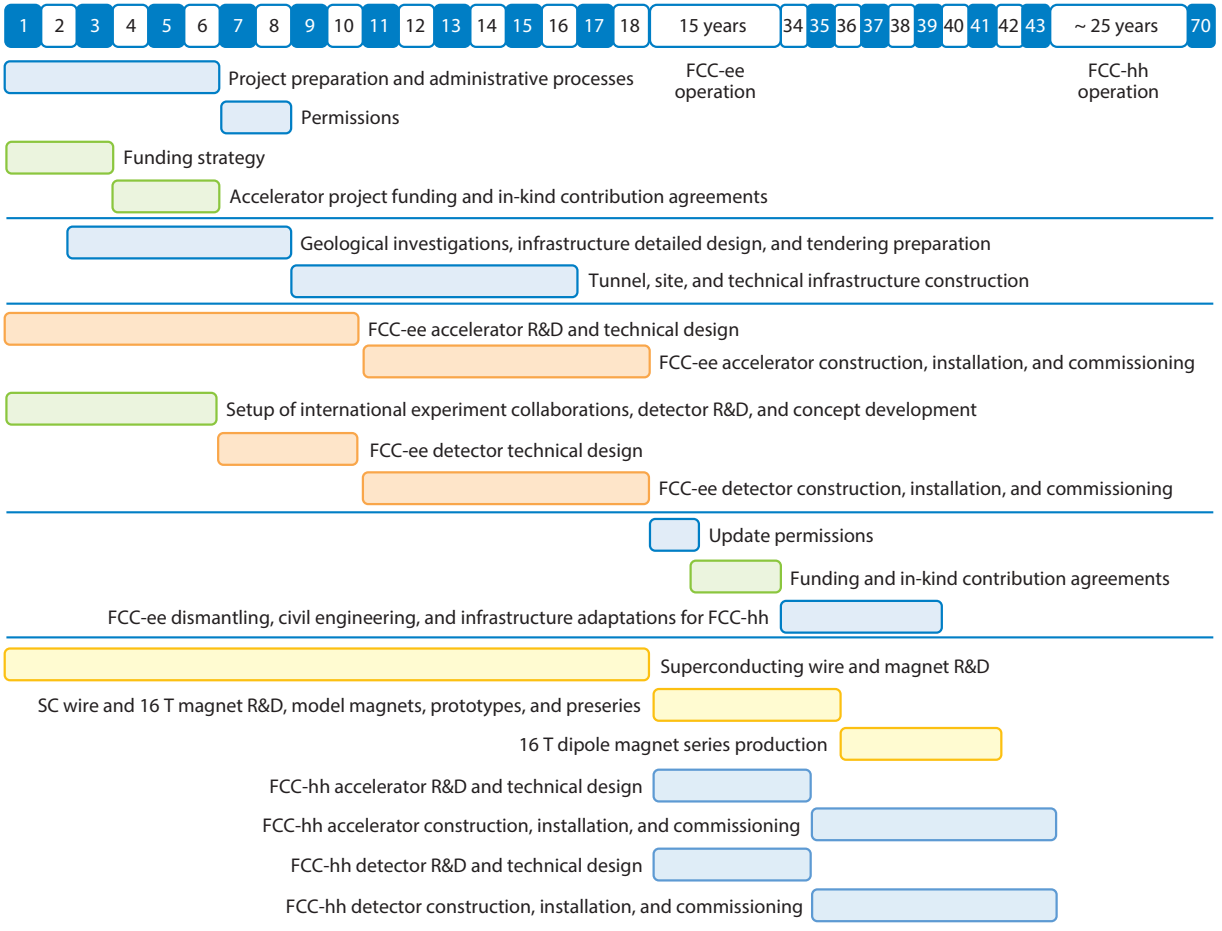

Figure 13

Overview of the implementation timeline for the integrated FCC program. Numbers in the top row indicate the year, starting at 1. Assuming a project decision around 2020, the first FCC-ee physics runs would be expected toward the end of the 2030s; physics operation for FCC-hh would begin in the 2060s. Abbreviations: FCC, Future Circular Collider; FCC-ee, FCC electron–positron collider; FCC-hh, FCC hadron collider; R&D, research and development.

The preparatory phase for the second stage, the energy-frontier hadron collider FCC-hh, will begin during the first half of the FCC-ee operation phase. After the end of FCC-ee operation, the FCC-ee machine will be removed, followed by installation and commissioning of the FCC-hh machine and detector, which will take about 10 years in total. The subsequent operation of the FCC-hh facility is expected to last 25 years, resulting in a total of 35 years for construction and operation of FCC-hh.

Host states: Switzerland and France are the two host states of CERN

The preparatory phase for each of the two project stages will include

- all administrative procedures with the host states, ultimately leading to construction permits and the provision of the required surface and underground rights-of-way;
- consultation process with authorities and public stakeholders;
- development of project financial, organizational, and governing structures; and
- site investigations, civil engineering design, and tendering for consultant and construction contracts.

The construction phase for the first stage, FCC-ee, will include

- all underground and surface structures required for FCC-ee;
- technical infrastructure; and
- FCC-ee accelerator, detectors, and associated injectors, including hardware checkout and beam commissioning.

The construction phase for the second stage, FCC-hh, will include

- removal of the FCC-ee machine and detectors;
- building of additional civil structures and adaptation of technical infrastructure for FCC-hh; and
- installation of the FCC-hh accelerator, injector, and detectors, including hardware and beam commissioning.

The staged implementation provides a time window of 25–30 years for R&D on key technologies for FCC-hh. **Figure 13** presents the timeline of the integrated FCC scenario.

SUMMARY POINTS

1. The FCC study is preparing for a post-LHC collider complex at CERN with a circumference of approximately 100 km.
2. The e^+e^- collider FCC-ee can be built with existing technology. Construction is expected to begin around 2028. Physics operation could then begin around 2039, seamlessly continuing the physics frontier program at CERN after the end of the HL-LHC project.
3. The FCC-ee will be an exceptional factory of Z, W, and Higgs bosons and of the top quark. It would search for small deviations from the SM in the coupling strengths between particles, as well as look for rare decays. The FCC-ee measurements would be sensitive to new particles at energies of up to tens of TeV. The FCC-ee physics program is staged, covering five different energies. The entire program FCC-ee could be executed over 15 years.
4. The future hadron collider FCC-hh will have a proton–proton collision energy of 100 TeV, almost 10 times that of the LHC. FCC-hh could begin to replace the FCC-ee in the second half of the 2050s. It will deliver an integrated luminosity at least five times higher than that of the HL-LHC (or 50 times that of the LHC).
5. The high-field magnets for the FCC-hh are under development in a worldwide R&D program.
6. The overall FCC program will extend over 7 decades or longer, through the end of the twenty-first century.

FUTURE ISSUES

1. Civil engineering studies will continue and a tunnel implementation plan will be prepared in close coordination with the host states.
2. A global governance structure will need to be established.

3. A full technical design of the e^+e^- collider FCC-ee will be developed.
4. The main R&D line for the 100 TeV hadron collider will consist of cost-efficient high-field magnets, based either on Nb_3Sn wire or on a high-temperature superconductor.

DISCLOSURE STATEMENT

The authors are not aware of any affiliations, memberships, funding, or financial holdings that might be perceived as affecting the objectivity of this review.

AUTHOR CONTRIBUTIONS

A. Blondel, P. Janot, M. Klein, M. Mangano, M. Mccullough, and W. Riegler contributed to the physics review in Section 2; M. Benedikt, V. Mertens, K. Oide, W. Riegler, D. Schulte, and F. Zimmermann contributed to the accelerator review in Sections 3–6. M. Benedikt and F. Zimmermann assembled the overall document.

ACKNOWLEDGMENTS

This review summarizes results from the international FCC Collaboration (see **https://cern.ch/fcc**). We are grateful to all collaboration members for their excellent and enthusiastic contributions. The research that led to this publication has received funding from the European Union's Horizon 2020 Research and Innovation program under grant numbers 654305 (EuroCirCol), 764879 (EASITrain), 730871 (ARIES), and 777563 (RI-Paths) and from the Seventh Framework Programme under grant number 312453 (EuCARD-2). The information herein reflects only the views of its authors. The European Commission is not responsible for any use that may be made of the information.

LITERATURE CITED

1. Mangano M, et al. *Future Circular Collider: Conceptual Design Report*, vol. 1: *Physics Opportunities*. Report CERN-ACC-2018-0056, CERN, Geneva (2018)
2. Benedikt M, et al. *Future Circular Collider: Conceptual Design Report*, vol. 2: *The Lepton Collider* (*FCC-ee*). Report CERN-ACC-2018-0057, CERN, Geneva (2018)
3. Benedikt M, et al. *Future Circular Collider: Conceptual Design Report*, vol. 3: *The Hadron Collider (FCC-hh)*. Report CERN-ACC-2018-0058, CERN, Geneva (2018)
4. Cepeda M, et al. *Higgs Physics at the HL-LHC and HE-LHC*. Report CERN-LPCC-2018-04, CERN, Geneva (2018)
5. Abe T, et al. arXiv:1011.0352 [physics.ins-det] (2010)
6. Oide K, et al. *Phys. Rev. Accel. Beams* 19:111005 (2016)
7. Richter B. *Nucl. Instrum. Methods A* 136:47 (1976)
8. Raimondi P, Shatilov D, Zobov M. arXiv:physics/0702033 (2007)
9. Raimondi P, Shatilov D, Zobov M. In *Proceedings of the 2007 IEEE Particle Accelerator Conference* (*PAC07*), p. 1469. Piscataway, NJ: IEEE (2007)
10. Boscolo M, Burkhardt H, Sullivan M. *Phys. Rev. Accel. Beams* 20:011008 (2017)
11. Aiba M, et al. *Nucl. Instrum. Methods A* 880:98 (2018)
12. Behnke T, et al. arXiv:1306.6327 [physics] (2013)

13. Linear Collid. Board. *Conclusions on the 250 GeV ILC as a Higgs factory proposed by the Japanese HEP community*. Report, Linear Collid. Board/Int. Comm. Future Accel., Fermi Natl. Accel. Lab., Batavia, IL. **http://icfa.fnal.gov/wp-content/uploads/LCB-Short-Conclusion-Nov2017.pdf** (2017)
14. Fujii K, et al. arXiv:1710.07621 [hep-ex] (2017)
15. Aicheler M, et al. *A multi-TeV linear collider based on CLIC technology*. Yellow rep. CERN-2012-007, CERN, Geneva (2012)
16. Boland MJ, et al. *Updated baseline for a staged Compact Linear Collider*. arXiv:1608.07537 [physics] (2016)
17. CEPC-SPPC Study Group. *CEPC-SPPC Preliminary Conceptual Design Report*, vol. 2: *Accelerator*. Report IHEP-CEPC-DR-2015-01, Inst. High Energy Phys., Beijing (2015)
18. CEPC-SPPS Study Group. *CEPC-SPPC Preliminary Conceptual Design Report*, vol. 1: *Physics and Detector*. Report IHEP-CEPC-DR-2015-01, Inst. High Energy Phys., Beijing (2015)
19. CEPC Study Group. arXiv:1809.00285 [physics] (2018)
20. Blondel A, et al. arXiv:1208.0504 [physics] (2011)
21. TLEP Des. Study Work. Group. *J. High Energy Phys.* 01:164 (2014)
22. Gianfelice E. *Phys. Rev. Accel. Beams* 19:101005 (2016)
23. Koratzinos M, Blondel A, Gianfelice-Wendt E, Zimmermann F. arXiv:1506.00933 [physics] (2015)
24. Tkaczuk J, Millet F, Duval J-M, Rousset B. *Phys. Rev. Accel. Beams* 20:041001 (2017)
25. Karpov I, Calaga R, Shaposhnikova E. *Phys. Rev. Accel. Beams* 21:071001 (2018)
26. Apollonio A, et al. *FCC-ee operation model, availability, and performance*. Paper presented at ICFA Advanced Beam Dynamics Workshop (eeFACT2018), 62nd, Hong Kong, Sept. 24–27 (2018)
27. Migliorati M, Belli E, Zobov M. *Phys. Rev. Accel. Beams* 21:041001 (2018)
28. Belli E, et al. *Phys. Rev. Accel. Beams* 21:111002 (2018)
29. Baikov AY, Marrelli C, Syratchev I. *IEEE Trans. Electron Devices* 62:3406 (2015)
30. Milanese A. *Phys. Rev. Accel. Beams* 19:112401 (2016)
31. Schaumann M. *Phys. Rev. Accel. Beams* 18:091002 (2015)
32. Mentink M, et al. *Phys. Rev. Accel. Beams* 19:111001 (2016)
33. Salmi T, et al. *Phys. Rev. Accel. Beams* 20:032401 (2017)
34. Benedikt M, Schulte D, Zimmermann F. *Phys. Rev. Accel. Beams* 18:101002 (2015)
35. Niemi A, et al. *Phys. Rev. Accel. Beams* 19:121003 (2016)
36. Besana MI, et al. *Phys. Rev. Accel. Beams* 19:111004 (2016)
37. Tahir NA, et al. *Phys. Rev. Accel. Beams* 19:081002 (2016)
38. Bartmann W, et al. *Phys. Rev. Accel. Beams* 20:031001 (2017)
39. Barna D, et al. *Phys. Rev. Accel. Beams* 20:041002 (2017)